



# Photovoltaic potential and land-use estimation methodology



Nuria Martín-Chivelet\*

CIEMAT, Avda. Complutense, 40, 28040 Madrid, Spain

## ARTICLE INFO

### Article history:

Received 20 May 2015

Received in revised form

16 October 2015

Accepted 18 October 2015

Available online 21 November 2015

### Keywords:

Photovoltaic potential

Packing factor

Land use

## ABSTRACT

This paper aims at improving the clarity and coherence of PV (photovoltaics) technical potential assessment, that is, calculation of the electricity that can be supplied by large-scale deployment of PV systems. A step-by-step method, compiling the main variables and processes involved, and including the packing factor in the technical potential equations, is proposed for this purpose. The influence of latitude and some design parameters, such as the shading criterion and tilt angle is analyzed. The paper supplies easy-to-use tools for estimating technical PV potential, as well as PV system land-use requirements. Analytical expressions and graphic examples, and a comparison of some case studies with existing PV plant data are included.

© 2015 Elsevier Ltd. All rights reserved.

## 1. Introduction

Renewable energy sources are essential to mitigating global warming and ensuring long-term energy stability, while awareness of the huge potential share of PV (photovoltaics) is continually increasing. According to a recent report by the International Renewable Energy Association [1], the technology has now developed to the point where the cost of PV power is becoming competitive with conventional electricity generation technologies in some scenarios, and is increasing its share of the energy mix around the world, with 175.3 GW installed at the end of 2014 [2]. But what are the possibilities of the photovoltaic technology? What is its potential share in the energy mix in each region? And how much land is needed for this technology compared to other energy sources?

In recent decades, studies have assessed the potential of photovoltaic energy for such different purposes as comparing the power capacity, power production or land use of energy sources, or boosting large-scale deployment of solar energy. Our review of the literature found different types of potential: theoretical, technical, economic and implementation. Some authors also include geographic potential in the classification [3–5], although it is implicit in the technical potential referred to by other authors. However, not all studies assess its economic or implementation potential.

All the references agree with the term *theoretical potential*, which refers to the estimated yearly horizontal solar irradiation in the area under study. There are different approaches for estimating solar irradiation on the ground, based on data from meteorological stations, on images from geostationary satellites, or a combination of both, which is currently the most common. For instance, Meteonorm [6], which is a global meteorological database used in several PV software applications, such as PVSyst [7], based on the interpolation of ground measurements supported by satellite images, PVGIS [8–10], which combines a solar radiation model with interpolated information from ground data available from the European Solar Radiation Atlas [11], HelioClim-3, based on the Heliostat2 method [12], recently upgraded by Heliostat4 [13], which contains surface solar irradiance from 15-min Meteosat image assessments, and the NASA Surface Meteorology and Solar Energy Program [14], which supplies average data from 1983 to 2005 satellite measurements for any cell in a  $1^\circ \times 1^\circ$  worldwide grid.

The *geographic potential* is defined as the fraction of the theoretical potential that is usable, in other words, the solar irradiation received on the land available for the PV facility. The area of this usable land is calculated by a *suitability factor* which is found considering a variety of different geographical constraints. At this point, it is crucial to distinguish between ground and building PV facilities, because the corresponding geographical constraints are quite different. Several methodologies have been proposed to assess the PV potential on roofs and facades. The effective available photovoltaic roof ratio is estimated in each case as a function of the building typology, usually ranging from 0.15 [15,16] to 0.4 [17–20], and in some cases over 0.5 [21,18]. Other authors, like Mainzer et al.

\* Tel.: +34 913466531.

E-mail address: [nuria.martin@ciemat.es](mailto:nuria.martin@ciemat.es).

[4], distinguish between flat roofs and slanted roofs, and propose suitability factors of 0.27 and 0.58, respectively, for buildings in Germany. Many studies use GIS (Geographic Information System) tools combined with aerial photogrammetric data and local descriptive information to build local Digital Surface Models using the LIDAR (Light Detection and Ranging) methodology. This approach can find the roof slope, orientation and shadows, and the irradiance it receives [22,23]. Studies are usually done for a specific region or municipality. However, some show wider approaches, and assess area suitability on a more global scale [24,17].

The constraints on ground PV plants mainly depend on the type of land use. Sorensen [24] proposed three types of suitability constants for ground PV applications in nonurban areas: 0% for bio-reserves and forests, 1% for agriculture, scrublands, savannah, tundra and grasslands, and 5% for extensive grasslands and deserts. Aware of the difficulty of a more precise approach, some authors have assumed this simplification [3] or other similar rules of thumb, such as Held [25], who based on Eurostat data [26], considered 0.5% of the total agricultural area suitable for centralized PV.

Explicit consideration of the geographic potential is often avoided, although it is always implicit in the *technical PV potential*, the term used by most authors, which is not always defined and calculated the same way. Hoogwijk [3] defines it as the geographic potential reduced by the losses associated with solar-to-electric power conversion. Mainzer [4] defines it as the technically usable irradiation, while IRENA [5] explicitly includes the constraint requirements related to large-scale facilities and technological, structural, ecological, and legislative restrictions in the term's definition. A similar approach is assumed by Greenpeace [27].

The *technical PV potential* is the actual usable solar energy or power once it has been transformed into electricity by PV systems. In the literature, it is given in terms of energy, or in terms of power (either peak power or nominal power), and sometimes both are supplied, although not always related to each other clearly enough. For instance, Singh and Banerjee [20] perform a detailed assessment of the daily estimated PV energy in Mumbai and give the final technical potential in terms of installed power, 2190 MW.

The key is to identify the parameters and assumptions in each case, which are usually more clearly expressed in the corresponding formulas used for the calculations. The simplest expression considers only the geographic potential multiplied by a rule-of-thumb effective conversion efficiency, such as 10% or 15% [3,24], and assumes that the PV modules are placed horizontally, so that all the available area is covered with PV modules. Further steps are taken by considering the PV modules in other positions, and plane-of-array irradiance [9], evaluating the efficiencies of the PV generator and the rest of the system separately, and estimating the effect of the ambient temperature and irradiance on PV module efficiency [20]. Another further step includes deducting shading losses from the direct radiation received by the PV modules, and calculating hourly energy produced [23]. There are also simpler approaches, such as quantifying the energy potential by the energy that a 1-kW peak system would generate in a given region using only locally received irradiation [9].

Several studies can be found on PV system land use dealing with its impact. The US National Renewable Energy Laboratory (NREL) [28] reports an exhaustive analysis of nearly 200 PV plants in the United States, showing land use for various PV system configurations based on capacity and electricity generation. Continuing a previous study [29], it distinguishes between total (all land enclosed by the site boundary) and direct area (land directly occupied by solar arrays, access roads, substations, service buildings and other infrastructure) in a PV plant. The average direct land use per unit of nominal power was 2.2 ha/MW<sub>AC</sub> for fixed-tilt PV

and 2.5 ha/MW<sub>AC</sub> for single-axis tracking PV. This is slightly higher than the 1.5 ha/MW<sub>AC</sub> for fixed-tilt PV systems and 2.1 ha/MW<sub>AC</sub> for single-axis tracking systems found by Denholm and Margolis [30], but quite similar to the Mai et al. [31] estimate of 2.0 ha/MW<sub>AC</sub>. Horner and Clark [32] and Fthenakis and Kim [29] evaluated the land use in terms of annual energy: 1.5 ha/GWh/yr, and 1.1 ha/GWh/yr, respectively.

However, it is not easy to find data in the literature about the area directly occupied by PV arrays in PV facilities, that is, the area of the PV generator. This is of interest because the PV generator area can be related to the installed PV module area, and thus to the PV power capacity, which is a relationship dependent on variables such as the PV module technology, the tilt angle of the array or inter-array spacing, all of which are important PV facility design parameters. Nevertheless, terms such as *PF* (packing factor) [28,32,33], *spacing factor* [5], *ground cover ratio* [34,35] and *occupation factor* [23] are used in the literature to refer to PV generator land occupation. While packing factor and ground cover ratio refer to the ratio between the PV array and the total ground area required for PV array installation, spacing factor and occupation factor refer to the inverse, the ratio between the ground or roof area necessary to install the PV modules and the area actually occupied by the installed PV modules.

A review of the packing factors of 63 PV plants distributed around the US [28] (from about latitudes 21° N to 45° N) shows wide variation of 13%–92%. While fixed-tilt systems have a capacity-weighted average packing factor of 47%, it is reduced to 34% in single-axis tracking systems and 25% in two-axis systems. This means a decrease of around 28% in the *PF* in single-axis systems and 47% in two-axis systems, compared to the fixed-tilt position. Several other references on local optimization designs deal with *PF* calculations. For example Lorenzo et al. [36] analyzed an azimuth-axis tracking system in northern Spain (42° N) in detail, and found an optimized *PF* of 18%, which is 40% lower than the fixed one.

Nevertheless, no explicit expression of the packing factor has been found in any of the formulations of the technical potential in PV potential studies, when such a term would enable the influence of different design parameters on PV potential to be assessed.

## 2. Approach

After a review of the literature, it may be concluded that, although many studies have assessed the photovoltaic potential, their methodologies, magnitudes and reporting units lack homogeneity, which leads to misunderstanding and makes it difficult to compare results. Furthermore, the packing factor has been identified as a key parameter relating area available and installed PV module area, and enabling a sensitivity analysis of the PV technical potential in different design parameters to be performed. Despite its usefulness, the packing factor does not explicitly appear in expressions of the technical potential.

The method proposed seeks to improve the clarity and coherence of PV technical potential assessment, by finding the main variables and processes involved step-by step, and including the packing factor in the technical potential equation. This will make it easier to study the influence of different design criteria on the PV technical potential.

### 2.1. Peak power and nominal power

Before explaining the steps in estimating the PV technical potential, the main characteristics of a PV system should be reviewed. The most important part is the PV generator, which is made up of all the PV modules grouped in arrays. In a PV plant, the modules are

usually mounted at a fixed angle facing the Equator, or they can be mounted on a one or two-axis solar tracking device to follow the sun position. The systems also include power conditioning devices, mainly inverters, which convert the DC (direct-current) generated by PV into AC (alternate-current) suitable to be fed into the grid. PV systems may also contain batteries, although most current PV plants do not have energy storage.

The PV module power is mainly influenced by irradiance, and to a lesser extent, by temperature:

$$P = P_0 \cdot \frac{G}{G_0} \cdot (1 - \gamma \cdot (T_c - T_{c,0})) \quad (1)$$

where  $G$  denotes global irradiance,  $T_c$  module temperature ( $c = \text{PV cell}$ ), and the subscript 0 stands for any reference situation. There are other second-order influencing parameters, such as the angle of incidence, surface soiling or the solar spectrum, that modify the PV module output parameters [37,38].

The *peak power* ( $P_p$ ) of a PV system is the nominal power of its PV generator, the sum of the nominal power of every PV module it is comprised of. Nominal power is rated at STC (standard test conditions): 1 kW/m<sup>2</sup>, cell temperature of 25 °C, and AM1.5 solar spectrum (the standard global spectrum related to an air mass of 1.5) [39,40]. The peak power of a PV system depends on module efficiency, size and number. The PV module's efficiency is the ratio of power density supplied by the module to the solar irradiance it receives.

Although there are variations among manufactures, each PV technology has a typical efficiency range. Table 1 shows the usual efficiencies of several current commercial PV technologies (average minimum and maximum) and the highest reported efficiencies in each technology to date [41]. The table also includes the module area needed to reach a reference peak power of 1 kW. Notice that module technology has an important role in the land area needed for a required peak power. The higher the efficiency, the less land is needed for the same plant capacity.

The *nominal power* of a PV system usually refers to the nominal AC output of the inverter, or the sum of the nominal power of each of them. When necessary, to distinguish whether a reported PV system power refers to the peak or nominal power, the corresponding unit symbol is shown by a  $p$  or AC subscript, respectively, for instance kW<sub>p</sub> or kW<sub>AC</sub>. In grid-connected systems the inverter nominal power is frequently similar to the PV generator peak power. Nevertheless, optimal inverter sizing depends on site insolation and array position, both of which affect the effective nominal power the inverter works at.

## 2.2. Generated PV electricity

PV plants having the same peak power may differ very significantly in the energy they generate over time, mainly due to the difference in solar irradiation received by the PV modules at each

site. The annual irradiation on the plane of the array,  $I_a$ , normalized by the reference irradiance of 1 kW/m<sup>2</sup>, is called the *reference yield* ( $Y_r$ ), and is expressed in units of hours [42], enabling comparison of the effective number of *peak hours* in each case.

The productivity of a grid-connected PV plant, usually calculated on a yearly basis, is characterized by the *final system yield* ( $Y_f$ ), which is the energy generated by the system normalized by the installed peak power (kWh/kW<sub>p</sub>), and may be interpreted as the effective number of plant production hours. In Spain, for instance, realistic production hours in fixed-array PV plants installed more than a decade ago normally vary from 900 to 1200 kWh/kW<sub>p</sub> [43], while values in the UK typically vary from 300 to 650 kWh/kW<sub>p</sub> [44]. Differences in PV plant yields are mainly due to differences in reference yields, and to a lesser degree, to differences in performance ratios.

The *PR* (*performance ratio*) is the ratio of the final system yield to the reference yield [42], and compares the energy actually generated with what is produced under the same amount of irradiation, but under ideal *no-losses* condition. Usually, PV system losses are due to array temperature, solar spectrum, angular reflection, surface soiling, wiring, and other PV system component inefficiencies or failures during operation. Although some of these losses should be calculated hourly, at least a final yearly integrated value has to be supplied to calculate the performance ratio. Thus:

$$PR = (1 - L_{temp}) \cdot (1 - L_{soiling}) \cdot (1 - L_{wiring}) \cdot (1 - L_{inverter}) \dots \quad (2)$$

The *PR* is useful for finding the efficiency of a PV system, regardless of module efficiency. Annual *PR* of recent PV systems is typically around 0.8 with an upward trend from around 0.7 in the 80 s [44].

## 2.3. Shading losses and effective irradiation

PV plant design should include an estimate of the system loss percentage due to shading, and limit the hours at which these losses occur. Although power loss from shading is commonly assumed to be proportional to the shaded area of the PV generator over time [45,46], the fact is that shading losses are actually higher, and are strongly influenced by the electrical configuration of the PV modules and generator (for instance, if part of a series-connected string of PV modules is shaded, the result is the same as if the whole string were shaded). The electrical and thermal effects of partial shading in PV modules have been widely studied [47–49]. A good review of early research on this subject was done by Woyte et al. [50].

Shading losses in the energy calculation can be quantified by a shading factor that modifies the total irradiance received by the PV generator. In a study comparing the energy yield of PV systems with different tracking strategies and packing factors, Narvarte and Lorenzo [34] considered two extreme effects of shading on

**Table 1**

Typical efficiency ( $\eta$ ) ranges of commercial flat-plate PV modules (average minimum and maximum) and maximum reported efficiencies at the date of writing (July 2015 [41]), and the PV module area required per kW-peak (kW<sub>p</sub>).

Technology	$\eta$ (%)			Required PV module area (m <sup>2</sup> ) per kW <sub>p</sub>		
	Avg min	Avg max	Max [41]	Avg max	Avg min	Min [41]
Monocrystalline silicon (m-Si)	15	17	22.9	6.7	5.9	4.4
Multicrystalline silicon (mc-Si)	14	16	18.5	7.1	6.3	5.4
Cadmium Telluride (CdTe)	11	13	17.5	9.1	7.7	5.7
Amorphous silicon, triple junction (a-Si)	7	9		14.3	11.1	
Copper/Indium/Gallium/Selenide (CIGS)	11	13	17.5	9.1	7.7	5.7
Amorphous silicon, tandem (a-Si/nc-Si)	9	11	12.3	11.1	9.1	8.1

estimated energy: power reduction equal to the shaded fraction, and any shade reduces power to zero. They assumed that shading affects only the direct and circumsolar components of the solar irradiance and calculated its hourly effect over one year. This approach has also been taken by other authors [23].

It is useful to integrate the effect of shading over the annual energy supplied by means of a shading factor,  $F_S$ , so that  $(1-F_S)$  accounts for the ratio of irradiation that effectively reaches the PV generator. An analysis of sensitivity [35] illustrates the influence of the packing factor on yearly shading losses with different tracking systems. In addition to type of tracking, the PV array aspect ratio (length/width) and field layout geometry play important roles in most tracking systems (except horizontal E–W single-axis). This analysis also shows how the same shading losses lead to packing factors of up to three times higher in fixed PV plants than in two-axis plants in the latitudes considered. At low to mid latitude, results become site-independent.

#### 2.4. Land use

The land required by a PV facility can be associated with the PV power installed or the PV energy generated. The power-based direct land use ( $DLU_P$ ) is defined as the area occupied per unit of installed power, while energy-based direct land use ( $DLU_E$ ) is defined as the area occupied per unit of generated energy. For potential assessment purposes, it can be assumed that the direct land area corresponds to area suitable for a PV facility,  $A_S$ . The area covered by the PV generator ( $A_{GEN}$ ), which is the area directly occupied by the PV arrays and the distances between them, is a fraction of the suitable area. The ratio between both areas is defined as the generator-to-system area ratio,  $GSR$ :

$$GSR = A_{GEN}/A_S \quad (3)$$

$GSR$  is dependent on the size and shape of the terrain and should be analyzed on a case by case basis. Nevertheless, a review of representative PV plants with nominal power over 1 MW shows that  $GSR$  typically ranges from 0.70 to 0.85.

### 3. Methodology

#### 3.1. Theoretical, geographical and technical potentials

The theoretical potential is calculated directly as the annual horizontal irradiation in the area under study,  $I_a(0)$ :

$$\text{Theoretical PV Potential (Energy)} = I_a(0) \cdot \text{Total Area} \quad [\text{kWh}] \quad (4)$$

The suitable area  $A_S$  is compared to the total area (suitability factor) to calculate the geographic potential, defined as the fraction of the theoretical potential that is usable:

$$\begin{aligned} \text{Geographic PV Potential (Energy)} \\ &= \text{Theoretical PV potential (Energy)} \cdot \text{Suitability factor} \quad [\text{kWh}] \\ &= I_a(0) \cdot A_S \quad [\text{kWh}] \end{aligned} \quad (5)$$

The suitable area is assumed to be occupied 100% by a PV system. This is called the direct land area, defined by the NREL [28] as the area occupied by the solar arrays, access roads, substations, service buildings and other infrastructure.

However, the theoretical and geographic potential models and expressions are outside the scope of this study.

The technical potential can be calculated in terms of capacity (installed power) or generated electricity (energy).  $PVPP$  (PV power potential) and  $PVEP$  (PV energy potential) are defined as the PV power per unit of land area and the PV energy per unit of land area, respectively. Observe that these two parameters estimate the potential in relative terms (power or energy per unit of area), and enable assessment of the absolute technical potential of the land or region in terms of power and energy:

$$\text{Technical PV Potential (Power)} = A_S \cdot PVPP \quad [\text{kW}] \quad (6)$$

$$\text{Technical PV Potential (Energy)} = A_S \cdot PVEP \quad [\text{kWh}] \quad (7)$$

#### 3.2. Peak power and generated energy expressions

The installed power of a PV plant is a function of the total area of all PV modules ( $A_{PV}$ ) and their efficiency ( $\eta$ ):

$$P_p = \eta \cdot A_{PV} \cdot G_{STC} \quad (8)$$

Where  $G_{STC}$  stands for the irradiance at standard test conditions, which is  $1 \text{ kW/m}^2$ .

The energy generated annually by a PV system is found from the peak power  $P_p$  of the system, the reference yield  $Y_r$ , the shading factor  $F_S$  and the performance ratio  $PR$ :

$$E_{PV} = P_p \cdot Y_f \cdot (1 - F_S) \quad (9)$$

Including the final system yield definition:

$$Y_f = Y_r \cdot PR \quad (10)$$

The expression for generated energy becomes:

$$E_{PV} = P_p \cdot Y_f \cdot (1 - F_S) \quad (11)$$

Alternatively, considering the annual irradiation on the plane of array  $I_a$ , instead of  $Y_r$ , and using Equation (6), the annual PV energy generated is calculated as:

$$E_{PV} = \eta \cdot A_{PV} \cdot I_a \cdot PR \cdot (1 - F_S) \quad (12)$$

#### 3.3. PV power potential and PV energy potential expressions

The expression of  $PVPP$  is obtained from that of  $P_p$  (see Equation (8)) and the suitable area  $A_S$ :

$$PVPP = \eta \cdot A_{PV} \cdot G_{STC} / A_S \quad (13)$$

The  $PF$  (packing factor) is defined as the ratio of the total PV array area to the actual land area occupied by all the PV arrays:

$$PF = A_{PV} / A_{GEN} \quad (14)$$

Taking into account the equation for  $GSR$  (see Equation (3)), the PV power potential may be expressed as a function of the packing factor  $PF$ , the generator-to-system area ratio  $GSR$  and PV module efficiency  $\eta$ :

$$PVPP = PF \cdot GSR \cdot \eta \cdot G_{STC} \quad (15)$$

Then the expression for the PV energy potential is:

$$PVEP = PF \cdot GSR \cdot \eta \cdot I_a \cdot PR \cdot (1 - F_S) \quad (16)$$

Or:

$$PVEP = PVPP \cdot Y_f \cdot (1 - F_S) \quad (17)$$



The variables and steps in *PVPP* (PV power potential) and *PVEP* (PV energy potential) estimation are summarized in Fig. 1.

Observe the importance of PV module efficiency (see Table 1 for typical ranges) to which PV potential is directly proportional.

In addition, as a result of differences in system yields at different sites, PV energy potential can also differ by over 100% for the same kind of PV system. The type of array positioning, whether tracking or fixed systems, may also significantly affect *PVEP*. In general, tracking systems show higher system yields than fixed, but lower power potentials due to lower packing factors.

### 3.4. Land use expressions

Land use can be found directly from *PVPP* and *PVEP*, as they are defined as the inverse of *PVPP* and *PVEP*, respectively:

$$DLU_P = (PVPP)^{-1} = (PF \cdot GSR \cdot \eta \cdot G_{STC})^{-1} \quad (18)$$

$$DLU_E = (PVEP)^{-1} = (PF \cdot GSR \cdot \eta \cdot I_a \cdot PR \cdot (1 - F_S))^{-1} \quad (19)$$

$DLU_P$  and  $DLU_E$  can be expressed in ha/MW and ha/(GWh/year), respectively.

### 3.5. Calculating the packing factor

The packing factor is an important parameter for calculating both *PVPP* and *PVEP*. Its value is a function of the PV array tilt angle, or sun-tracking type, and the array aspect ratio, land characteristics, and the shading criterion chosen, which determines the distance between arrays in each case.

#### 3.5.1. Determining the tilt angle

The optimum tilt angle,  $\beta_{opt}$ , for fixed PV modules should be accurately determined for each application and location. For grid-connected ground PV systems, the target is usually to harvest the

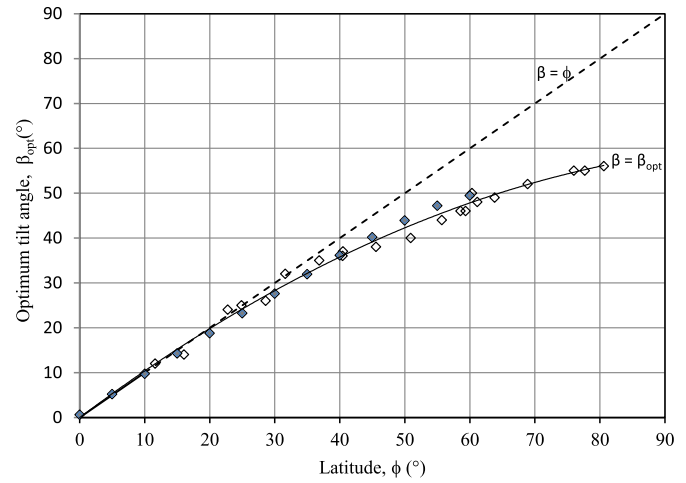


Fig. 2. Optimum tilt angle ( $\beta_{opt}$ ) over latitude ( $\phi$ ) and fitted polynomial curve found with PVSystem [7] at different sites (empty diamonds), and with calculated reference [52] data (solid diamonds). The dashed straight line corresponds to tilt angle = latitude.

highest possible irradiation during the year to maximize yearly PV generation. Although the particular climate conditions at each site also affect the optimization of the tilt angle, the latitude is the most determinant variable.

Fig. 2 shows the optimum tilt angle for sites at different latitudes calculated with PVSystem [7] and using reference [52] data. All the data are fitted to a quadratic function of latitude, resulting in coefficient of determination  $R^2 = 0.993$ .

$$\beta_{opt} = -0.0049 \phi^2 + 1.0888 \phi \quad (20)$$

The difference between the latitude and the optimum tilt angle is nearly zero at sites close to the Equator, and increases gradually

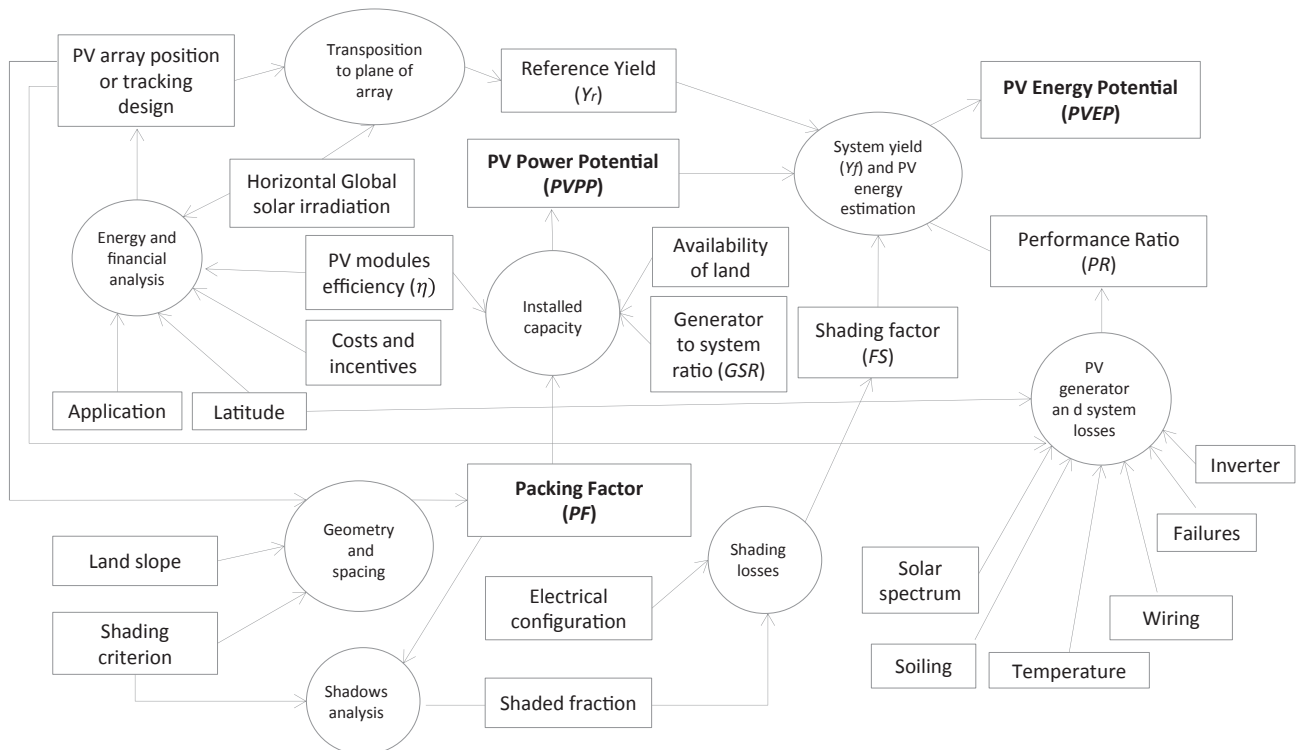


Fig. 1. Flow diagram of PV power potential and PV energy potential estimation. Circles represent processes. Rectangles show input data and parameters.

with latitude, to around  $10^\circ$  at latitudes near  $60^\circ$  (see Fig. 2). Many different numerical models for the calculation of the optimum tilt angle have been suggested in different regions [46,51–53]. A common default assumption is to consider the tilt angle similar to the latitude,  $\beta_{lat}$ , which has been shown to be a good approximation up to approximately  $30^\circ$  latitude, as shown below.

Many large grid-connected photovoltaic plants include solar tracking to increase solar energy collection. In this sense, two-axis tracking is the most efficient solution, although single-axis options (polar, horizontal and vertical) usually lead to higher final cost-effective results [54].

### 3.5.2. Shading losses criteria and minimum inter-row distance

General PV plant design rules, such as avoiding any inter-row shading around noon throughout the year, which means assuring it at the winter solstice, are usually taken to reduce shading when irradiance is highest and, consequently, power reduction and hot-spot phenomena become more critical. While the condition of avoiding shading only at noon could be enough at latitudes above  $50^\circ$ , where solar irradiance is very low around winter solstice, it would be insufficient at lower latitudes, where it is recommended to avoid shading for 4 h around noon (noon  $\pm$  2 h), see for example, the Spanish recommendations for grid connected PV systems [52]. In the present paper, both shading criteria are considered, labeled Shading Criteria 1 and 2, respectively (sc1, sc2).

The sun elevation is calculated from the Earth's declination  $\delta$ , the latitude  $\phi$ , and the hour angle  $\omega$ :

$$\sin \gamma_S = \sin \delta \sin \phi + \cos \delta \cos \phi \cos \omega \quad (21)$$

And the sun azimuth is calculated from the equation:

$$\sin \psi_S = (\sin \gamma_S \sin \phi - \sin \delta) / (\cos \gamma_S \cos \phi) \quad (22)$$

Fig. 3 is a schematic diagram showing the minimum distance between arrays necessary to avoid shading as given by

$$d = l \cos \beta + \frac{l \sin \beta}{\tan \gamma_S} \cos \psi_S \quad (23)$$

At the winter solstice, the declination is  $-23.45^\circ$ . Furthermore, for Shading Criterion 1:

$$\omega = 0 = \psi_S; \quad \gamma_S = \sin^{-1}[\cos(\sin(\phi - \delta))] \quad (24)$$

So for sc1, the expression for the minimum distance between array rows is:

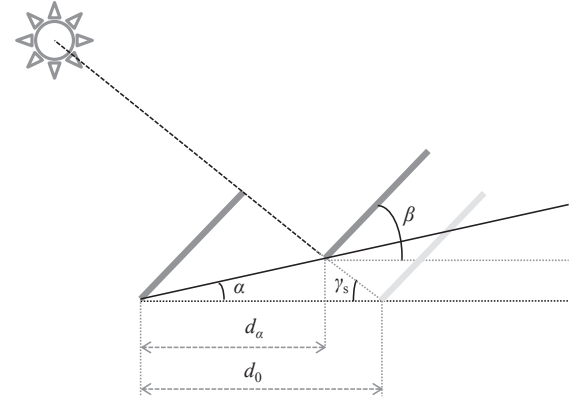
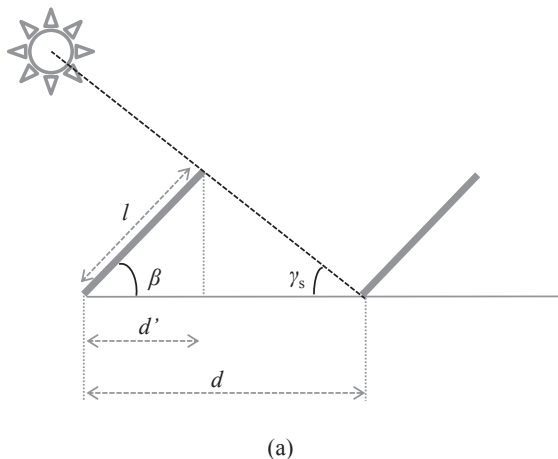


Fig. 4. Minimum distance between rows considering shading criterion sc1, on flat land sloped at an angle  $\alpha$  towards the Equator ( $d_\alpha$ ), compared to the minimum distance if the land were horizontal ( $d_0$ ).

$$d = l \cos \beta + \frac{l \sin \beta}{\tan(66,55 - \phi)} \quad (25)$$

### 3.5.3. Sloped land

A large area of flat land makes installation simpler and cheaper. However, when the ground is sloped toward the Equator, the minimum distance between rows decreases with the inclination of the land, making it possible to achieve higher packing factors in the installation, and thereby, more power capacity per unit of area. If the land is sloped at an angle  $\alpha$ , the inter-row distance  $d_\alpha$  decreases with regard to the one for horizontal land,  $d_0$  (Equation (23)). Considering Shading Criterion 1, the following formula relates both minimum distances (see Fig. 4):

$$d_\alpha = d_0 \left[ 1 + \frac{\tan \alpha}{\tan \gamma_S} \right]^{-1} \quad (26)$$

However, it should be taken into account that sloped lands are more susceptible to erosion, and this is the main reason why in general steeply sloping land should be avoided for PV installation.

### 3.5.4. The packing factor expression

The following expression for the packing factor on flat land is found from Equations (14) and (23) and Fig. 3:

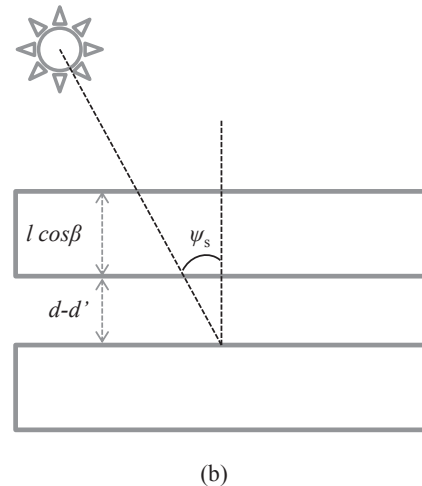


Fig. 3. (a) Sectional view of sun elevation and array tilt angle, and minimum distance between arrays to avoid shading. (b) Horizontal projected areas and solar azimuth angle.

$$PF = \frac{l}{d} = \left( \cos \beta + \frac{\sin \beta}{\tan \gamma_S} \cos \psi_S \right)^{-1} \quad (27)$$

where  $d$  may be  $d_0$  or  $d_\alpha$ . Observe that the packing factor for fixed PV arrays is not dependent on the dimensions of the PV modules, but only a function of latitude and tilt angle, for a given shading criterion. Notice that both tilt angles (similar to latitude or optimized) completely or mainly depend on latitude, so in the end, a good approximation of the packing factor could be determined by the latitude, as shown in the following section.

Equations (15)–(17) and Equation (27) lead to the analytical expressions for the PV power and energy potentials:

$$PVPP = \left( \cos \beta + \frac{\sin \beta}{\tan \gamma_S} \cos \psi_S \right)^{-1} \cdot GSR \cdot \eta \cdot G_{STC} \quad (28)$$

$$PVEP = \left( \cos \beta + \frac{\sin \beta}{\tan \gamma_S} \cos \psi_S \right)^{-1} \cdot GSR \cdot \eta \cdot I_a \cdot PR \cdot (1 - F_S) \quad (29)$$

#### 4. Analysis of packing factors in some case studies

The packing factors of different PV system designs have been calculated taking the abovementioned concepts and criteria into consideration. Fig. 5 shows the values found with different combinations of PV array positions and shading criteria plotted over latitude. Two tilt angles are taken for fixed PV modules, one the same as the latitude ( $\beta_{lat}$ ) and the other the optimized angle found by Equation (20) ( $\beta_{opt}$ ). An East–West horizontal single-axis tracking PV system is also compared. The two shading criteria selected are no shading only at noon (sc1) and no shading during 4 h around noon (sc2).

As expected, the packing factor constantly decreases with increase in latitude. In general, it is highest for fixed PV modules at optimum tilt angles with sc1. Table 2 summarizes the relative differences in packing factor percentage at the three array positions: fixed arrays with tilt optimized for maximum yearly production ( $PF_{opt}$ : solid lines in Fig. 5), fixed arrays with tilt angle equal to latitude ( $PF_{lat}$ : dashed lines in Fig. 5) and horizontal E–W single-

axis sun-tracking arrays ( $PF_{1ax}$ : dotted lines in Fig. 5). The significant influence of latitude in some cases, and the constant relative difference between  $PF_{lat}$  and  $PF_{1ax}$  may be observed.

Differences between  $PF_{opt}$  and  $PF_{lat}$  are not significant at latitudes under  $30^\circ$ , but gradually increase up to 11–13% at  $60^\circ$ . However, in absolute terms, differences between  $PF_{opt}$  and  $PF_{lat}$  never exceed two points. The single-axis tracking system leads to reductions of up to 22% in the packing factor compared to fixed systems (at  $60^\circ$  latitude), while in absolute terms, differences between  $PF_{opt}$  and  $PF_{1ax}$ , which are high at low angles (nine points at latitudes under  $10^\circ$ ) decrease significantly with latitude (seven points at  $30^\circ$ , and two points at  $60^\circ$ ).

In all cases, the more restrictive the shading criterion is, the lower the packing factor. This influence increases with latitude (relative differences up to 16% at  $50^\circ$  and 49% at  $60^\circ$  in fixed systems) and become especially significant in the tracking system (23% at  $50^\circ$  and 93% at  $60^\circ$ ). See Table 3.

Each curve plotted in Fig. 5 can be fitted to a quadratic function of latitude ( $\phi$ ), dependent on two fitting parameters,  $A$  and  $B$ :

$$PF = PF_0 - A \cdot \phi^2 - B \cdot \phi \quad (30)$$

where  $PF_0$  represents the packing factor at  $0^\circ$  latitude, which is 100% for a fixed system on flat land, and depending on the shading criterion, 92.4% or 91.5% for a horizontal E–W single-axis system. Fitted parameters  $A$  and  $B$  in each case, along with the regression coefficients indicating good data fit are shown in Table 4. Observe that although in all cases  $A \ll B$ ,  $A$  multiplies the square of the latitude, so the contributions of both terms to the  $PF$  are comparable.

As shown, the packing factor of a PV plant on flat horizontal land has a limit of 100%. In contrast, Fig. 6 shows some examples of the variation in the packing factor with latitude and land slopes varying from 0% (horizontal) to 100% ( $45^\circ$ ) (Equations (26) and (27)). It should be mentioned that these curves represent theoretical calculations, steeply sloping land should be avoided to reduce soil erosion, although these results can be useful for PV installation on buildings' roofs.

#### 5. Calculating PV potentials and land use

The packing factors calculated above may lead to quite different PV power potentials, depending on the PV technology (see Equation (13) and Table 1). Table 5 shows calculated  $PVPP$  for fixed systems with PV modules at the optimal tilt, with four different configurations determined by the combination of the module efficiency, generator-to-system area ratio and the shading criterion.

Observe that  $PVPP$  varies from 0.1 MW/ha to 1.6 MW/ha, at latitudes from  $0^\circ$  to  $60^\circ$ . With a PV module efficiency of 15% and  $GSR$  of 0.75, it is comparable to what was found in the review of literature on existing PV plants (see Table 6). The differences are due mainly to different  $\eta$ ,  $GSR$  and  $PF$ .

**Table 2**  
Relative differences in packing factors for different PV plant designs.

Latitude ( $^\circ$ )	$PF_{opt} - PF_{lat} / PF_{opt}$ (%)		$PF_{lat} - PF_{1ax} / PF_{lat}$ (%)		$PF_{opt} - PF_{1ax} / PF_{opt}$ (%)	
	sc1	sc2	sc1	sc2	sc1	sc2
0	0	0	8.3	9.0	8.3	9.0
10	0	0	8.3	9.7	8.1	9.5
20	0.3	0.3	8.3	10.1	8.5	10.4
30	1.5	1.7	8.3	10.4	9.6	11.9
40	3.6	4.1	8.3	10.5	11.6	14.2
50	6.8	7.7	8.3	10.6	14.5	17.4
60	11.3	12.7	8.3	10.6	18.6	21.9

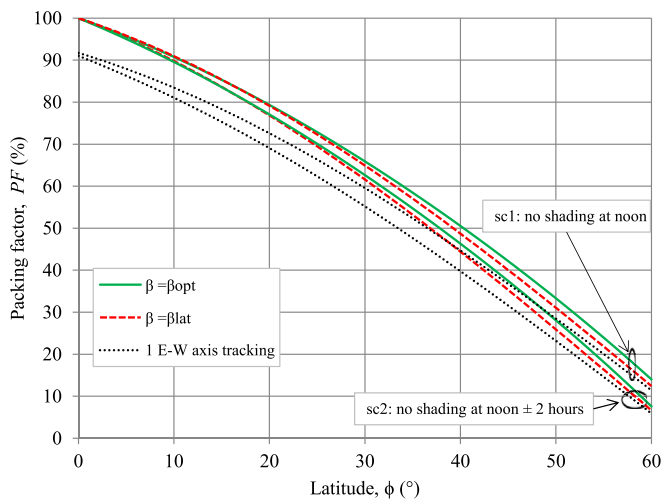


**Fig. 5.** Packing factors found using two different types of fixed array tilt angles (optimum for a maximum yearly production and equal to latitude) and E–W horizontal single-axis tracking. A complete set of curves is shown for each of the two shading criteria.

**Table 3**

Relative differences in power factors for each type of PV plant design for the two shading criteria, sc1 and sc2.

Latitude (°)	$PF_{lat}^{sc1} - PF_{lat}^{sc2} / PF_{lat}^{sc1}$ (%)	$PF_{opt}^{sc1} - PF_{opt}^{sc2} / PF_{opt}^{sc1}$ (%)	$PF_{1ax}^{sc1} - PF_{1ax}^{sc2} / PF_{1ax}^{sc1}$ (%)
0	0.0	0.0	0.8
10	1.3	1.3	3.0
20	2.9	2.9	5.1
30	5.2	5.0	7.9
40	8.9	8.4	12.4
50	16.6	15.7	22.9
60	46.7	45.9	92.6

**Table 4**Fit parameters of the quadratic dependence of the packing factor (in percentage) with latitude (in degrees), see Equation (30), for two fixed PV systems, horizontal East–West tracking and the two types of shading criteria. The coefficient of determination ( $R^2$ ) of each regression is also included.

	$PF_{lat}^{sc1}$	$PF_{lat}^{sc2}$	$PF_{opt}^{sc1}$	$PF_{opt}^{sc2}$	$PF_{1ax}^{sc1}$	$PF_{1ax}^{sc2}$
A	0.0104	0.0099	0.0100	0.0098	0.0089	0.0075
B	0.8552	0.9803	0.8366	0.9505	0.8295	0.9873
$R^2$	0.9998	0.9997	1.0000	0.9995	0.9997	0.9884

Assuming a reference yield of 1800 h, a shading factor of 0.05 and a performance ratio of 0.8, and the results shown in Table 5,  $PVEP$  varies from 958 to 1362 MWh/year/ha at 30° latitude, and from 735 to 1045 MWh/year/ha at 40°.  $PVEP$  tolerance margins for comparison with the published data are wider (see Table 6) due to additional differences in performance ratio, shading factors and, especially, reference yields.

Fig. 7 shows the direct land use calculated at different sites with different latitudes and reference yields taken from the [7] database. The PV modules are positioned at the optimum fixed tilt and the inter-row distance avoids shading during the four central hours of the day (sc2). The performance conditions are the same in all cases, for simplification ( $\eta = 15\%$ ,  $GSR = 0.8$ ,  $PR = 0.8$ ,  $F_s = 0.05$ ). Results are plotted in Fig. 7 together with three hypothetical curves of  $DLU_E$ , calculated with three constant values of  $Y_r$ . Observe that lines corresponding to 1600 h and 2500 h fade as latitude increases. This indicates that although climate conditions also affect  $Y_r$ , the latitude establishes an upper reference limit, so that high reference yields

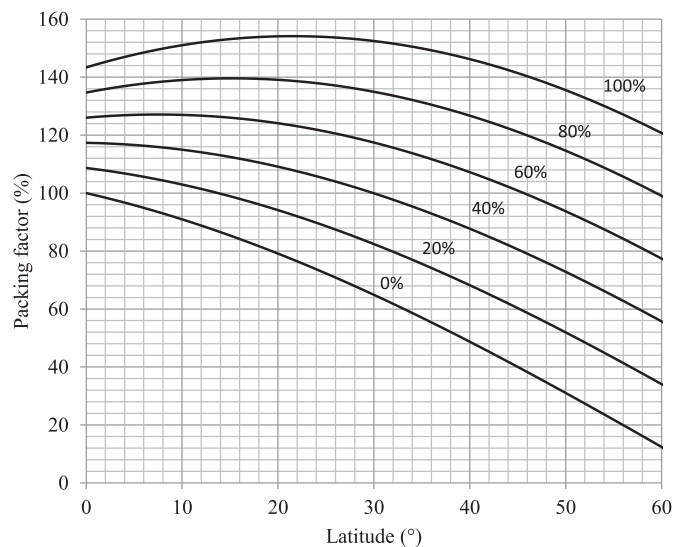


**Fig. 6.** Variation in the packing factor with land slope and latitude, if PV arrays are fixed at the optimum tilt angle and separated by shading criterion 1 on flat land tilted towards the Equator. A 100% slope corresponds to 45° tilt.

such as 2500 h are not found at 60°. However, low-latitude sites may have relatively low reference yields, as in Bogota.

Notice the growing significant influence of latitude from medium latitudes on, compared to the influence of local irradiation. The reason is that land use increases asymptotically with latitude, as it varies inversely with the packing factor, which decreases as a quadratic function of latitude (see Equation (30)).

## 6. Conclusions

This paper provides a methodology and some mathematical and graphical tools for estimating PV potential and land use. The methodology includes calculation steps and some key parameters, such as the packing factor, which depends on the latitude, PV array tilt angle, type of tracking, inter-row shading criterion and slope of the land. Some typical design criteria are included to illustrate the influence of these parameters in the packing factors obtained. The two tilt angles taken for fixed PV modules are common in PV plants and flat roofs: one is the same as the latitude ( $\beta_{lat}$ ) and the other is the optimized angle ( $\beta_{opt}$ ), which was shown to be a simple function of latitude. An East–West horizontal axis single-tracking PV system was also compared using two selected shading criteria, no shading only at noon (sc1) and no shading for 4 h around noon (sc2).

Analytical expressions were obtained for the packing factor and the PV potential using these two design shading criteria. Packing factors were then calculated under different conditions and the results were fitted to a simpler  $PF$  analytical expression, which approximates a quadratic decrease as a function of latitude. Differences using  $\beta_{lat}$  or  $\beta_{opt}$  are not significant up to 30°, while the single-axis system always leads to significantly lower packing factors. For instance, depending on the latitude, they are 12%–22% lower than those found with the fixed optimum tilt with shading criterion sc2. In all cases, inclusion of this shading criterion leads to lower packing factors than sc1, especially for tracking systems at higher latitudes. In such cases a sensitivity study for the particular conditions is recommended to determine the best solution.

The expression for the packing factor makes it easy to calculate the  $PVPP$  (PV power potential),  $PVEP$  (PV energy potential) and

**Table 5**PV power potential for each latitude indicated, at optimal tilt and with different combinations of  $\eta$ ,  $GSR$  and shading criteria (sc1 and sc2).

Latitude (°)	$PVPP$ (MW/ha)			
	$\eta = 15\%, GSR = 0.75$		$\eta = 20\%, GSR = 0.80$	
	sc1	sc2	sc1	sc2
0	1.13	1.13	1.60	1.60
10	1.02	1.01	1.45	1.43
20	0.89	0.87	1.27	1.23
30	0.74	0.70	1.05	1.00
40	0.57	0.52	0.81	0.74
50	0.37	0.32	0.53	0.45
60	0.16	0.09	0.22	0.12



**Table 6**

PV installed power and yearly PV generated energy per hectare obtained from the review of the literature, for comparison with calculated *PVPP* and *PVEP*, respectively.

	MW/ha	MWh/year/ha
Ong et al. [28]: fixed, $P < 20$ MW	0.45	772
Ong et al. [28]: 1-axis, $P < 20$ MW	0.39	852
Ong et al. [28]: 2-axis, $P < 20$ MW	0.26	603
Ong et al. [28]: fixed, $P > 20$ MW	0.43	797
Ong et al. [28]: 1-axis, $P > 20$ MW	0.27	883
Mai et al. [31]	0.50	
Denholm and Margolis [30]: fixed	0.65	
Denholm and Margolis [30]: 1-axis	0.48	
Horner and Clark [32]		650
Fthenakis and Kim [29]		915

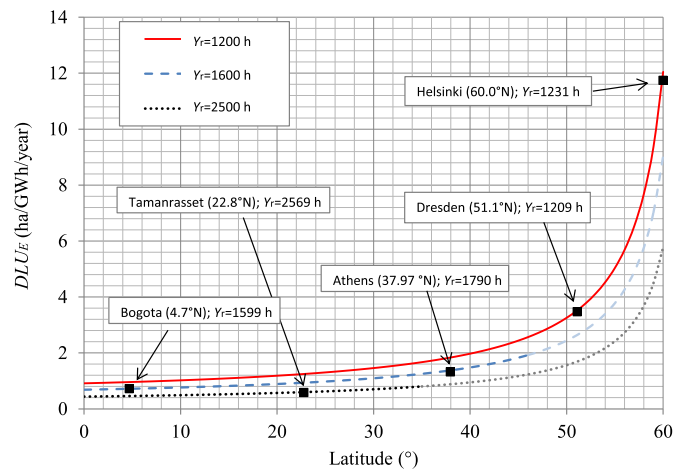


**Fig. 7.** Direct land per unit of annual energy generated by a PV plant with fixed arrays at optimal tilt,  $\eta = 15\%$ ,  $GSR = 0.8$ ,  $PR = 0.8$  and  $F_5 = 0.05$ . Dots show local reference yields, and curves show unreal constant reference yields at the latitude. Lines fade at unreal combinations of latitude and reference yield.

land-use requirement ( $DLU_P$  and  $DLU_E$ ). A new parameter, generator-to-system area ratio  $GSR$ , is proposed for estimating *PVPP*, in addition to the packing factor and PV module efficiency. For a PV module efficiency of 15%, *PVPP* varies from 0.1 MW/ha to 1.6 MW/ha, at latitudes from 0° to 60°. At mid latitudes, it is comparable to real data found in the literature. Differences can be explained by existing margins in PV module efficiencies and design parameters. On the other hand, the *PVEP* found shows wider variation, mainly due to the additional dependence on the reference yield. Nevertheless, results are also comparable to the reported data found in the literature.

Calculation of the land requirement from the proposed *PVPP* and *PVEP* mathematical expressions is straightforward. Direct land use, like the packing factor and PV potentials, is very latitude dependent.  $DLU_E$  increases asymptotically with latitude, although it decreases inversely proportional to the reference yield. Direct land use was calculated at several different sites to illustrate both influences.

## References

- [1] IRENA. Renewable power generation costs in 2014. 2015.
- [2] IRENA. Renewable energy capacity statistics 2015. 2015.
- [3] Hoogwijk MM. On the global and regional potential of renewable energy sources [Doctoral thesis]. 2004. Utrecht.
- [4] Mainzer K, Fath K, McKenna R, Stengel J, Fichtner W, Schultmann F. A high resolution determination of the technical potential for residential-roof-mounted photovoltaic systems in Germany. *Sol Energy* 2014;105:715–31.
- [5] IRENA. Estimating the renewable energy potential in Africa a GIS-based approach working report. 2014.
- [6] Meteornorm7. Global meteorological database. <http://meteornorm.com/> [accessed August 2015].
- [7] Mermoud A. PVSYST software v6.24. PVsyst SA. 2014.
- [8] Huld T, Suri M, Dunlop E. A GIS-based system for performance assessment of solar energy systems over large geographical regions. In: *Solar 2006 Conference: Renewable Energy, key to climate recovery*, July 7–13; 2006. Denver CO, USA.
- [9] Sári M, Remund J, Cebecauer T, Dumortier D, Wald L, Huld T, et al. First steps in the cross-comparison of solar resource spatial products in Europe. In: *Proc. EUROSUN 2008 1st International Conference on Solar Heating, Cooling and Buildings*; Lisbon, Portugal; October 7th–10th; 2008.
- [10] Sári M, Huld TA, Dunlop ED, Ossenbrink HA. Potential of solar electricity generation in the European Union member states and candidate countries. *Sol Energy* 2007;81:1295–305 [accessed July 2015]. <http://re.jrc.ec.europa.eu/pvgis/>.
- [11] Scharmer K, Grief J. ESRA. European solar radiation atlas. 4th ed. Paris: Les Presses de l'Ecole des Mines; 2000.
- [12] Rigollier C, Lefèvre M, Wald L. The method Heliosat-2 for deriving shortwave solar radiation from satellite images. *Sol Energy* 2004;77(2):159–69. <http://dx.doi.org/10.1016/j.solener.2004.04.017>.
- [13] Espinar B, et al. In: *HelioClim-3: a near-real time and long-term surface solar irradiance database COST-WIRE-ES1002: Workshop May 22nd–23rd*; 2012. p. 53–61. Roskilde, Denmark.
- [14] NASA SSE. Surface meteorology and solar energy release 6.0 surface meteorology and solar energy (SSE) release 6.0 methodology version 3.1.2. 2014 [accessed August 2015]. <https://eosweb.larc.nasa.gov/sse/>.
- [15] Theodoridou I, Karteris M, Mallinis G, Papadopoulos AM, Hegger. Assessment of retrofitting measures and solar systems' potential in urban areas using geographical information systems: application to a Mediterranean city. *Renew Sustain Energy Rev* 2012;16(8):6239–61.
- [16] Bergamasco L, Asinari P. Scalable methodology for the photovoltaic solar energy potential assessment based on available roof surface area: application to Piedmont Region (Italy). *Sol Energy* 2011;85(5):1041–55.
- [17] Gutschner M, Nowak S, Ruoss D, Toggweiler P, Shoen T. Potential for building integrated photovoltaics. International Energy Agency Report IEA-PVPS T7-4. 2002.
- [18] Yue CD, Huang GR. An evaluation of domestic solar energy potential in Taiwan incorporating land use analysis. *Energy Policy* 2011;39(12):7988–8002.
- [19] Izquierdo S, Rodrigues M, Fueyo N. A method for estimating the geographical distribution of the available roof surface area for large-scale photovoltaic energy-potential evaluations. *Sol Energy* 2008;82:929–39.
- [20] Singh R, Banerjee R. Estimation of rooftop solar photovoltaic potential of a city solar Energy, vol. 115; 2015. p. 589–602. <http://dx.doi.org/10.1016/j.solener.2015.03.016>.
- [21] Scartezini JL, Montavon M, Compagnon R. Computer evaluation of the solar energy potential in an urban environment. In: *Eurosun 2002 Conference*, Bologna (Italy); 2002.
- [22] Caamaño-Martín E, Higuera E, Neila J, Useros I, Masa-Bote D, Tortora F, et al. Solar potential calculation at city and district levels. *Proc Sustain City VII WIT Trans Ecol Environ* 2012;155.
- [23] Verso A, Martin A, Amador J, Dominguez J. GIS-based method to evaluate the photovoltaic potential in the urban environments: the particular case of Miraflores de la Sierra. *Sol Energy* 2015;117:236–45. <http://dx.doi.org/10.1016/j.solener.2015.04.018>.
- [24] Sørensen B, Kuemmel B, Meibom P. Long-term scenarios for global energy demand and supply: four global greenhouse mitigation scenarios, IMFUFA. Texts No. 359. Roskilde University Institute 2; 1999.
- [25] Held AM. Modelling the future development of renewable energy technologies in the European electricity sector using agent-based simulation [Doctoral thesis]. 2010. Karlsruhe.
- [26] Eurostat. In: *Total agricultural land*. Eurostat statistics. Luxembourg: European Commission; 2009.
- [27] Energy revolution. In: *A sustainable world energy outlook*, Global Wind Energy Council, European Energy Renewable Council and Greenpeace International; 2012. ISBN 978-9073361-92.
- [28] Ong S, Campbell C, Denholm P, Margolis R, Heath G. Land use requirements for solar power plants in the United States. National Renewable Energy Laboratory; June 2013. p. 39. Technical Report NREL/TP-6A20-56290.
- [29] Fthenakis V, Kim HC. Land Use and Electricity Generation: A Life-Cycle Analysis. *Renew Sustain Energy Rev* 2009;13:1465–74.
- [30] Denholm P, Margolis R. Land-Use Requirements and the Per-Capita Solar Footprint for Photovoltaic Generation in the United States. *Energy Policy* 2008;36(9):3531–43.
- [31] Mai T, Wiser R, Sandor D, Brinkman G, Heath G, Denholm P. Renewable Electricity Futures Study, Volume 1: exploration of high-penetration renewable electricity futures, National Renewable Energy Laboratory NREL/TP-6A20-52409. June 2012. p. 280.
- [32] Horner R, Clark C. Characterizing variability and reducing uncertainty in estimates of solar land use energy intensity. *Renew Sustain Energy Rev* 2013;23:129–37.
- [33] Hernandez RR, Hoffacker MK, Field CB. Land-Use Efficiency of Big Solar. *Environ Sci Technol* 2014;48:1315–23. <http://dx.doi.org/10.1021/es4043726>.
- [34] Narvarte L, Lorenzo E. Tracking and ground cover ratio. *Prog Photovolt Res Appl* 2008;16:703–14. <http://dx.doi.org/10.1002/pip.847>.

- [35] Gordon JM, Wegner HJ. Central-station solar photovoltaic systems: field layout, tracker, and array geometry sensitivity studies. *Sol Energy* 1991;46(4): 211–7.
- [36] Lorenzo E, Pérez M, Ezpeleta A, Acedo J. Design of tracking photovoltaic systems with a single vertical axis. *Prog Photovolt Res Appl* 2002;10:533–43.
- [37] Martín N, Ruiz JM. A new method for the spectral characterisation of PV modules. *Prog Photovolt Res Appl* 1999;7(4):299–310. [http://dx.doi.org/10.1002/\(SICI\)1099-159X](http://dx.doi.org/10.1002/(SICI)1099-159X).
- [38] Martín N, Ruiz JM. Calculation of the PV modules angular losses under field conditions by means of an analytical model. *Sol Energy Mater Sol Cells* 2001;70(1):25–38. [http://dx.doi.org/10.1016/S0927-0248\(00\)00408-6](http://dx.doi.org/10.1016/S0927-0248(00)00408-6).
- [39] International Electrotechnical Commission, 2005 International Electrotechnical Commission. IEC 61215:2005. Crystalline silicon terrestrial photovoltaic (PV) modules – design qualification and type approval
- [40] International Electrotechnical Commission, 2008 International Electrotechnical Commission. IEC 61646:2008. Thin-film terrestrial photovoltaic (PV) modules – design qualification and type approval
- [41] Green MA, Emery K, Hishikawa Y, Warta W, Dunlop ED. Solar cell efficiency tables (version 46). *Prog Photovolt Res Appl* 2015;23:805–12. <http://dx.doi.org/10.1002/pip.2637>.
- [42] International Electrotechnical Commission, 1998 International Electrotechnical Commission. IEC 61724:1998. Photovoltaic system performance monitoring – guidelines for measurement, data exchange and analysis
- [43] Lorenzo E. La energía que producen los sistemas fotovoltaicos conectados a red: el mito del 1300 y el cascabel del gato. *Era Sol* 2002;107:22–8.
- [44] Nordmann T, Clavdetscher L, Van Sark W, Green M. Analysis of long-term performance of PV systems, Report IEA-PVPS T13-05:2014. 2014.
- [45] Deline C. Partially shaded operation of a grid-tied PV system. In: *Proc. 34th IEEE Photovoltaic Specialists Conf*; 2009. p. 1268–73.
- [46] Government of Spain. Instituto para la Diversificación y Ahorro de la Energía IDAE. Pliego de Condiciones Técnicas de Instalaciones Conectadas a Red. Progenisa Ed., ISBN 978-84-95693-62-4. [http://ida.electura.es/materia/solar\\_fotovoltaica/](http://ida.electura.es/materia/solar_fotovoltaica/) [accessed July 2015]
- [47] García M, Maruri JM, Marroyo L, Lorenzo E, Pérez M. Partial shadowing, MPPT performance and inverter configurations: observations at tracking PV plants. *Prog Photovolt Res Appl* 2008;16:529–36.
- [48] Alonso-García MC, Ruiz JM, Herrmann W. Computer simulation of shading effects in photovoltaic arrays. *Renew Energy* 2006;31:1986–93.
- [49] Quaschnig V, Hanitsch R. Shade calculations in photovoltaic systems. In: *Proc. ISES World Congress, Harare, 1995*; 1995.
- [50] Woyte A, Nijs J, Belmans R. Partial shadowing of photovoltaic arrays with different system configurations: literature review and field test results. *Sol Energy* 2003;74:217–33.
- [51] Darhmaoui H, Lahjouji D. Latitude based model for tilt angle optimization for solar collectors in the Mediterranean region. *Energy Procedia* 2013;42:426–35.
- [52] Skeiker K. Optimum tilt angle and orientation for solar collectors in Syria. *Energy Convers Manag* 2009;50:2439–48.
- [53] Cronemberger J, Caamaño-Martín E, Vega Sánchez S. Assessing the solar irradiation potential for solar photovoltaic applications in buildings at low latitudes – making the case for Brazil. *Energy Build* 2012;55:264–72. <http://dx.doi.org/10.1016/j.enbuild.2012.08.044>.
- [54] De Simon-Martin M, Alonso Tristan C, Díez-Mediavilla M. Performance indicators for sun-tracking systems: a case study in Spain. *Energy Power Eng* 2014;6:292–302.